Thermochimica Acta, 71 (1983) 365–372
Elsevier Science Publishers B.V., Amsterdam – Printed in The Netherlands

TRANSITION ENTROPIES AND MESOMORPHIC BEHAVIOUR OF *p-n*-ALKOXYBENZYLIDEN-*p*′-BUTOXYANILINES

DOMENICO GRASSO, CONCETTA GANDOLFO and SALVATORE FASONE

Istituto di Chimica e Chimica Industriale dell'Università di Catania, Viale A. Doria 8, 95125 Catania (Italy)

(Received 25 July 1983)

ABSTRACT

Calorimetric data on the mesogenic homologous series $H_9C_4OC_6H_4N{=}CHC_6H_4OC_nH_{2n+1}$ are presented. Trends in the nematic–isotropic liquid transition temperatures, enthalpies and entropies are briefly discussed. A remarkable polymorphism is evidenced in several compounds. The importance of the thermal history of the samples in relation to their thermal behavior is shown.

INTRODUCTION

Benzylidenaniline derivatives are of remarkable interest owing to their ability to give mesophases. In previous papers [1,2] we reported the thermodynamic data referring to the two series $H_5C_2OC_6H_4N{=}CHC_6H_4OC_nH_{2n+1}$ and $H_7C_3OC_6H_4N{=}CHC_6H_4OC_nH_{2n+1}$, respectively. In the present herein data referring to the series $H_9C_4OC_6H_4N{=}CHC_6H_4OC_nH_{2n+1}$, with $n = 1$–8 for compounds A–H, respectively.

The aim of these studies is to identify those molecular properties required for the existence of mesophases, through systematic variations of terminal substituents of a common central group; in this case benzylidenaniline.

The thermodynamic data are presented as supported by Gray and Winsor [3] in K, kcal mol^{-1}, and cal mol^{-1} K^{-1} for temperatures, T, enthalpies, ΔH, and entropies, ΔS, respectively.

EXPERIMENTAL

Materials

Commercially available amines and aldehydes were used for the synthesis of the compounds. Equivalent quantities of amine and aldehyde were dissolved in anhydrous benzene and refluxed for several hours. The water of

0040-6031/83/$03.00

reaction was removed azeotropically and the crude products so obtained were purified by several crystallizations at low temperature from anhydrous ethanol at constant melting point.

Differential scanning calorimetry (DSC)

A Mettler TA processor equipped with a DSC-20 measurement cell, previously calibrated for temperature and energy, using indium as the standard, was used for the measurements. Several DSC scans were carried out for each sample.

Thermal microscopy (TM)

The transition temperatures were observed using a Galileo polarizing microscope with a 20 × 0.22 objective and a Mettler FP 52 microfurnace for sample temperature control. Samples were mounted on a glass slide and covered with a glass cover slip. Special care was taken to ensure clear observation.

RESULTS AND DISCUSSION

In Table 1, the temperatures, the ΔH and the ΔS values relative to the phase transitions for all compounds are collected. The corresponding transition diagrams are reported in Fig. 1. Those reported as "cycle I" were obtained using samples purified and crystallized from anhydrous ethanol ("virgin products"); those indicated as "cycle II" were obtained using, as sample, the condensed product obtained by cooling from cycle I.

The transition temperatures refer to thermal microscopy measurements, where not otherwise specified. The DSC measurements were carried out on heating, or on cooling at 4 K $\min^{-1}$, where not otherwise specified. In order to obtain data on monotropic transitions, the procedure reported in ref. 2 was followed.

From an evaluation of the data reported, a different thermal behaviour of the compounds examined is evident. In particular, the following should be noted.

Compound A

The thermal behaviour of this compound shows a remarkable dependence on the heating rate. To this end, several measurements were carried out at scan rates of 0.2, 1, 2, ..., 10 K $\min^{-1}$. At a scan rate of 4 K $\min^{-1}$ (standard conditions), this compound presents, on heating, only a solid–isotropic liquid transition, while on cooling, a monotropic nematic appears before a solidification. In the following cycles, carried out under the same conditions, a new solid–solid transition appears on cooling. Moreover, the

TABLE 1

Thermodynamic data for compounds A–H

Compound	Transition	Cycle I			Cycle II		
		T	ΔH	ΔS	T	ΔH	ΔS
A	K_0-I	387.5	7850	20.25	387.5	7850	20.25
	I-N	381.4	160	≃ 0.4	381.4	160	≃ 0.4
	N-K_1	≃ 356.4[a]	6700	18.8	≃ 356.4[a]	6700	18.8
B	K_0-K_1	378.0	7695	≃ 20.0			
	K_1-K_2	382.0					
	K_2-N	384.8			384.8	4895	12.72
	N-I	405.8	≃ 270	0.66	405.8	≃ 240	≃ 0.6
	I-N	405.5[a]	≃ 270	0.66	405.5	≃ 290	≃ 0.7
	N-K_2	372.5[a]	4809	12.91	373.5[a]	4817	12.89
C	K_0-K_1	388.1	900	2.11			
	K_1-I	393.7	6705	17.08			
	K_2-I				393.7	6310	16.02
	I-N	388.0	187	0.48	388.0[a]	177	0.46
	N-K_2	381.3[a]	6110	16.0	381.3	6260	16.40
D	K_0-K_1	380.0[a]	≃1380	≃ 3.5			
	K_1-I	398.5	7350	18.44	398.5	7400	18.56
	I-N	395.5	≃ 320	0.78	395.5	≃ 260	0.66
	N-K_2	≃ 389.3[a]	≃ 6735	≃17.0	389.7[a]	≃ 6770	≃17.0
	K_2-K_3	388.8[a]			389.0[a]		
	K_3-K_4	385.2[a]	≃ 85	≃ 0.22	385.2[a]	≃ 85	≃ 0.22
E	K_0-K_1	375.0[a]					
	K_1-I	387.5	7400	19.04	388.6	7390	19.01
	I-N	387.5	270	0.7	387.5	≃ 270	0.7
	N-K_2	381.5[a]	7070	≃18.0	383.3	2580	6.73
	K_2-K_3	382.6[a]			383.7	4490	11.70
F	K_0-N	374.2	9100	24.3			
	K_2-N				374.2	7300	19.5
	N-I	390.5	≃ 340	0.87	390.5	≃ 350	0.89
	I-N	390.5	≃ 340	0.87	390.5	≃ 350	0.89
	N-K_1	371.0	5700	15.40	371.0	5700	15.4
	K_1-K_2[b]						
G	K_0-N	374.0	9540	25.46			
	K_2-N				374.6	9150	24.4
	N-I	386.9	≃ 300	≃ 0.7	386.9	≃ 300	≃ 0.8
	I-N	386.8	≃ 300	0.7	386.0	≃ 300	≃ 0.8
	N-S_1	368.2	≃ 7750	≃ 21.0	368.3	≃ 7750	≃ 21.0
	S_1-K_1	367.4			867.4		
	K_1-K_2	≃ 363.0			≃ 363.0		
H	K_0-N	381.6	10300	26.98	381.6	10300	26.98
	N-I	387.8	≃ 340	≃ 0.9	387.8	≃ 340	0.9
	I-N	387.7	≃ 450	≃1.2	387.7	≃ 450	≃1.2
	N-S_1	372.4	≃ 250	≃ 0.7	372.4	≃ 250	≃ 0.7
	S_1-K_1	361.0	8780	24.31	361.0	8780	24.31

[a] Temperature obtained by DSC measurements.

[b] Transition detectable by DSC measurements but non reproducible.

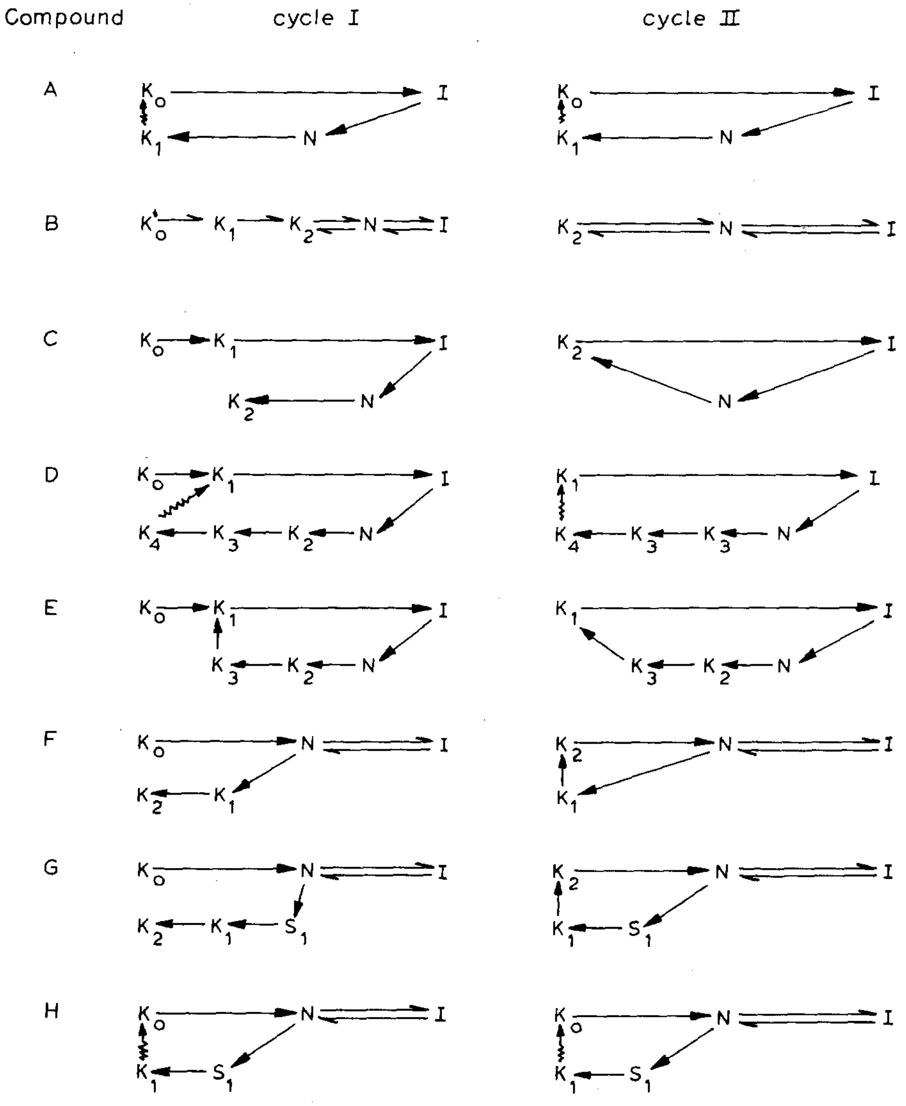

Fig. 1. Transition diagrams: K, solid; N, nematic phase; S, smectic phase; I, isotropic liquid.

data referring to the thermal cycles obtained at different heating rates, show three or four solid–solid transitions, at temperatures and with energies not reproducible, besides the monotropic nematic transition at about 108.3°C. These data are not reported in Table 1.

Compound B

This compound presents a remarkable thermal hysteresis. On first heating, a polymorphism with at least three solid phases appears with a total ΔH of 7700 cal mol^{-1}. In the following cycles, on heating, only one solid phase is evident with a $\Delta H \sim 4900$ cal mol^{-1}. The same value is obtained, within experimental error, for the ΔH corresponding to the nematic solid transition obtained on cooling. Measurements carried out at 0.2 K min^{-1} give comparable results. The solid phase, K_2, thermodynamically unstable, changes to the stable form very slowly. Many days are required for this transformation.

Compound C

This compound presents a remarkable thermal hysteresis; on heating the "virgin product", a solid–solid transition occurs with a remarkable value of ΔS, before clarification. In the following cycles, if carried out within a few hours from the first one, this solid–solid transition does not occur. Many days are required for the K_1–K_0 transformation.

On cooling, all cycles are coincident within the experimental error. Besides a monotropic nematic phase, two solid phases appear, at a scan rate of 4 K min^{-1}, while at 0.2 K min^{-1} four solid–solid transitions are evident. These transitions, which are not detectable by thermal microscopy measurements, are not reported in Table 1.

Compound D

The thermal history of this compound is remarkably affected by the scan rate. Moreover, the preceding phase is important in its characterization. A K_0–K_1 transition is evident on heating the "virgin product" before melting.

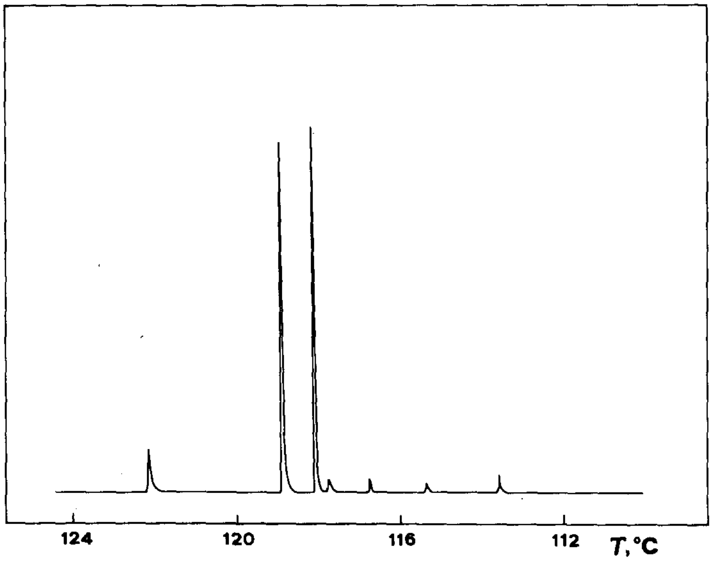

Fig. 2. DSC thermogram of *p*-*n*-butoxybenzyliden-*p*′-*n*-butoxyaniline (on cooling).

This transition does not appear in the following cycles which show, on heating, only a K_1–I.L. transition. On cooling, under standard conditions, besides the isotropic–nematic (monotropic) transition, at least three other transitions are evident. Only one of these is detectable by TM measurements. In order to obtain better information, a DSC scan was carried out at a scan rate of 0.2 K min^{-1}. Whilst on heating the thermogram maintained the features of the previous thermogram, on cooling, almost six crystalline phases besides the nematic phase (Fig. 2) are evident in the temperature range examined. The sum of the energies relative to these transitions is approximately equivalent to that obtained in the previous cycle carried out under standard conditions, where supercooling is observed.

Compound E

On heating the "virgin product", a solid–solid transition appears at about 375 K before clarification at 388.7 K. This K_0–K_1 transition does not appear in the following cycles, even if repeated at an interval of three days.

On cooling, under standard conditions, a monotropic nematic phase appears, followed by nematic–smectic and smectic–solid transitions, very close together, which, in the measurements carried out at 0.2 K min^{-1}, appear more distinct and quantitatively measurable.

Compound F

The data referring to this compound show a very large thermal hysteresis of the crystal–nematic transition ($\Delta H = 9100$ cal mol^{-1} on heating and 5700 cal mol^{-1} on cooling). Moreover, in the second cycle, the value of ΔH corresponding to the K–N transition (on heating), depends remarkably on the time elapsed between the actual measurements and the solidification of the preceding cycle. The datum reported in Table 1 ($\Delta H = 7300$ cal mol^{-1}) was obtained ~ 50 min after the preceding solidification N–K.

After the first cycle the system probably remains in a metastable phase which changes slowly into a thermodynamically stable phase. Measurements recorded at a scan rate of 1 K min^{-1} showed the presence of different solid–solid transitions.

Compound G

On heating, a stable nematic phase appears in the range 374.7–387 K. No other transitions are evident, in contrast with the data obtained by TM, where a further transition appears at 372.9 K.

On cooling, after the isotropic–nematic transition, the thermogram shows a very complicated structure. Almost three transitions are evident under standard conditions. Recording the thermogram at a scan rate of 1 K min^{-1}, a new shoulder appears. However, it was not possible to obtain the enthalpimetric values for each transition. The ΔH value reported in Table 1 refers to the overall transition. The second cycle differs from the first in having a small thermal hysteresis of the K–N transition.

Compound H

The thermal cycle of this compound shows a stable nematic phase on heating, and a monotropic smectic phase besides the nematic phase, on cooling. No remarkable differences appear between the thermodynamic data referring to the first and following cycles. Also the scan rate does not seem to affect the results. The values obtained under different conditions are equivalent, within the experimental error.

Figure 3 reports the trend of the total transition entropy referring to the first and second cycles (upper and lower curves, respectively). The compounds A, E and H present no thermodynamic hysteresis, unlike the other compounds. The remarkable polymorphism of all the compounds, which is evidenced by the presence of the numerous solid phases, is the probable cause of this hysteresis. The upper curve of Fig. 3 also shows an interesting even–odd alternation. Assuming the schematic molecular arrangement reported in ref. 4 for molecules of this kind, it can be seen that the termini of the chains of the compounds B, D, F and H allow the greatest intermolecular interactions. This means that the terminal C–C bonds of adjacent molecules are nearly parallel to each other. Moreover, the increasing trend of the total entropy against the chain length confirms that the stability of the compounds considered increases progressively with the length of the chains.

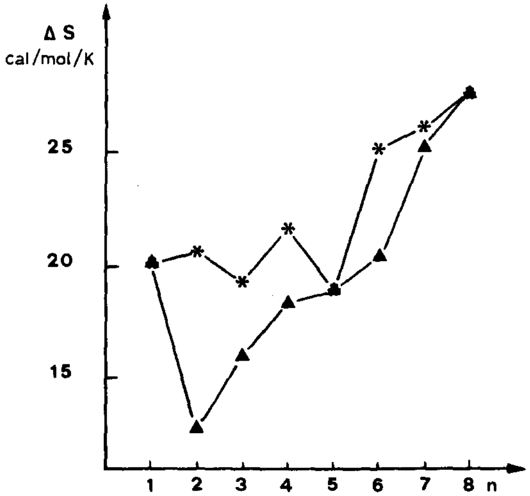

Fig. 3. Effect of alkyl chain length on the total transition entropy: *, cycle I; ▲, cycle II.

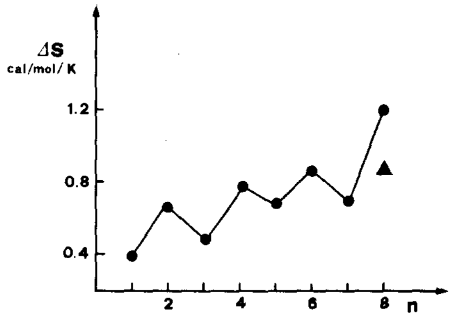

Fig. 4. Effect of alkyl chain length on the entropy of the liquid isotropic–nematic transition: ●, I–N transitions; ▲, N–I transition.

Figure 4 reports the trend for the isotropic liquid–nematic transition, referring to the first thermal cycle. Again, each case shows the characteristic even–odd effect and no appreciable overcooling is present, except for compound H. For this compound, Fig. 4 also reports the ΔS value referring to the isotropic liquid–nematic transition; this value is surprisingly higher than the value obtained in the N–I.L. transition. This experimental datum is confirmed in the second and following cycles and in different measurements carried out on different samples. This phenomenon is also shown by the compounds E, F, G and H of ref. 2. In each case a different thermodynamic stability of the nematic phase is evidenced if the nematic phase is obtained on heating or on cooling.

REFERENCES

1 D. Grasso, C. Gandolfo, L. Abate, G. Buemi and S. Fasone, Thermochim. Acta, 46 (1981) 71.
2 D. Grasso, L. Abate, C. Gandolfo and S. Fasone, Thermochim. Acta, 61 (1983) 227.
3 G.W. Gray and P.A. Winsor, Liquid Crystals and Plastic Crystals, Ellis-Horwood, Chichester, 1974.
4 C. Gandolfo and D. Grasso, Thermochim. Acta, 56 (1982) 59.